



Numerical simulation for regional ozone concentrations: A case study by weather research and forecasting/chemistry (WRF/Chem) model

Khandakar Md Habib Al Razi, Moritomi Hiroshi

Environmental and Renewable Energy System, Graduate School of Engineering, Gifu University, 1-1
Yanagido, Gifu City, 501-1193, Japan.

Abstract

The objective of this research is to better understand and predict the atmospheric concentration distribution of ozone and its precursor (in particular, within the Planetary Boundary Layer (Within 110 km to 12 km) over Kasaki City and the Greater Tokyo Area using fully coupled online WRF/Chem (Weather Research and Forecasting/Chemistry) model. In this research, a serious and continuous high ozone episode in the Greater Tokyo Area (GTA) during the summer of 14–18 August 2010 was investigated using the observation data. We analyzed the ozone and other trace gas concentrations, as well as the corresponding weather conditions in this high ozone episode by WRF/Chem model. The simulation results revealed that the analyzed episode was mainly caused by the impact of accumulation of pollution rich in ozone over the Greater Tokyo Area. WRF/Chem has shown relatively good performance in modeling of this continuous high ozone episode, the simulated and the observed concentrations of ozone, NO_x and NO₂ are basically in agreement at Kawasaki City, with best correlation coefficients of 0.87, 0.70 and 0.72 respectively. Moreover, the simulations of WRF/Chem with WRF preprocessing software (WPS) show a better agreement with meteorological observations such as surface winds and temperature profiles in the ground level of this area. As a result the surface ozone simulation performances have been enhanced in terms of the peak ozone and spatial patterns, whereas WRF/Chem has been succeeded to generate meteorological fields as well as ozone, NO_x, NO₂ and NO.

Copyright © 2013 International Energy and Environment Foundation - All rights reserved.

Keywords: Air quality modeling; WRF/Chem; Ozone concentrations, High ozone episode.

1. Introduction

Summer ozone [1], one of the criteria pollutants of major significance as per MOE (Ministry of Environment, Japan), is mainly formed by the oxidant process of volatile organic compounds (VOCs) in the presence of nitrogen oxides NO_x (NO and NO₂) and sunlight intensity. Studies over different regions clearly indicate that the ozone concentration is strongly dependent on locations due to the varied ambient chemical conditions in different regions, prevailing meso and micro meteorological conditions and the resulting wind flow and turbulence fields [2-5]. The industrial complexes are located in the Tokyo Bay area are the largest in Japan and are the major stationary sources of pollutants such Nitric Oxide (NO), Nitrogen Dioxide (NO₂), Oxide of Nitrogen (NO_x), Sulfur Oxides SO_x, hydrocarbons and aerosols etc.),

while Greater Tokyo Area is the largest contributor of pollutants from mobile sources. In addition the topography of this area is very complicated, which leads to complex wind pattern [6].

The main pollutants emitted into the atmosphere in urban areas are sulfur oxides (SO_x), nitrogen oxides (NO_x), carbon monoxide (CO), volatile organic compounds (VOCs), metal oxides, and particulate matter (PM/aerosols) mostly consisting of black carbon, sulfates, nitrates, and organic matter. The oxidation of CO, VOCs, and NO_x produces ozone in the planetary boundary layer (PBL), which has an important impact on human health in urban areas. The recent economic developments in China, Korea, and Japan are very rapid due to the rapid growth of heavy industrial operations. The rapidly growing urbanization in these countries will cause wide-ranging potential consequences in terms of environmental problems. These areas have been suffering from severe air pollution problems for the last decade, such as high particulate matter (PM) concentrations and poor visibility [7-10]. As industrial activity and the number of automobiles increase, the emission of volatile organic carbons (VOCs) and NO_x (NO + NO₂) will also significantly increase. Both VOCs and NO_x play critical roles in ozone formation in the troposphere [2, 11] and the variations in their concentrations and the ensuing effects on the ozone production rate can be characterized as either NO_x-sensitive or VOC-sensitive [11-14]. Thus, obtaining a better understanding of the relationship between ozone precursors (VOCs, NO_x) and ozone formation in East Asia is one of the critical pre-required pieces of information necessary to develop effective ozone control strategies [15-17].

In Japan, VOC, NO_x, and SO_x were categorized as hazardous air pollutants (HAPs) in 1996 and are on the list of Substances Requiring Priority Action published by the Central Environmental Council of Japan [18]. The Central Environmental Council published the second report on the "Future direction of measures against hazardous air pollutants" in October 1996. The second report also proposed that voluntary actions to reduce emissions, as well as investigations of hazards, atmospheric concentrations and pollution sources of those substances, should be promoted. Although industrial emissions of VOCs, NO_x, and SO_x in Japan have been decreasing in recent years, primarily due to voluntary reductions from industrial sources, the risks of exposure to these pollutants have remained largely unknown. In this study, a rapid change of ozone and its precursors were simulated during the spring of 2008. The simulation results contribute to a better understanding of ozone variability in coastal areas of the Sea of Japan [19]. A three-dimensional chemical/dynamical regional model (WRF/Chem V-3.3) was applied to analyze the causes of the rapid changes in ozone during this period.

Numerical models have been widely used in studying atmospheric mesoscale phenomena including air-pollution transport [20, 21]. They provide physically consistent flow field and prevailing high spatial meteorological fields for application in pollutant transport and diffusion in coastal regions [22]. Jin and Raman [23] studied dispersion from elevated releases under the sea-land breeze flow using a mesoscale dispersion model which included the effects of local topography, variability in wind and stability [23]. Simulation tools consisting mesoscale atmospheric models coupled to Lagrangian particle/Eulerian grid dispersion models have been developed to simulate the transport and diffusion of atmospheric pollutants in regions of complex topography and coastal conditions [24-27].

It is apparent that the use of WRF/Chem to predict the ozone concentration and its precursors in Japan domain is very rare. Chatani and Sudo [28] observed and analyzed the seasonal variation of ozone concentration in the Japan domain by using the WRF/Chem, CHASER model with monitoring station data during 1996-2005. They tried to evaluate the performance of the WRF/Chem, CHASER model with monitoring data during this period. Masanori et al. [29] evaluated vertical ozone profiles simulated by WRF/Chem using Lidar observation over the Kanto region of Japan in 27-29 July and 16-21 August 2005. Kurokawa et al. [30] showed the influence of meteorological variability on interannual variations of the springtime boundary layer ozone over Japan between 1981-2005. Kurokawa et al. [31] depicted an analysis of episodic pollution of photochemical ozone during 8-9 May 2007 over Japan using the nesting RAMS/CMAQ modeling system. Hayasaki et al. [32] described episodic pollution of photochemical ozone during 8-9 May 2007 over Japan. Saikawa et al. [33] analyzed the impact of China's vehicle emissions on regional air quality in 2000 and 2020. It is evident that the early research work on ozone simulation by WRF/Chem in the Japan domain did not show any time series ozone concentration with observation data to find out an high ozone episode.

In this study an attempt has been made to examine the evolution of surface ozone and other precursor emissions like NO, NO₂, NO_x in the Kawasaki City of Greater Tokyo Area using WRF/Chem, an online chemistry model. The performance of WRF/Chem in the simulation of ozone concentration distribution in the region that have occurred during the summer (middle of August) condition and the results from

this study could provide useful information about ozone formative meteorological processes to air quality regulatory agencies and health administrators. The summer climate in the study region is characterized with strong land-ocean thermal gradients and the resulting mesoscale sea breeze circulation. The concentration distributions of ozone in August 14-18, 2010 during the summer with sufficient observations were selected to assess the model performance.

2. Numerical modeling

2.1 Model description

The Weather Research and Forecasting (WRF) model is a mesoscale numerical weather prediction system designed to serve both operational forecasting and atmospheric research needs. The development of the WRF model has been a collaborative partnership, principally among the National Center for Atmospheric Research (NCAR), the National Oceanic and Atmospheric Administration (NOAA), the National Center for Environmental Prediction (NCEP), the Forecast Systems Laboratory (FSL), the Air Force Weather Agency (AFWA), the Naval Research Laboratory, Oklahoma University, and the Federal Aviation Administration (FAA). The WRF model is a fully compressible and Euler nonhydrostatic model. It calculates winds (u , v , and w), the perturbation potential temperature, the perturbation geopotential, and the perturbation surface pressure of dry air. It can also optionally output other variables, including turbulent kinetic energy, the water vapor mixing ratio, the rain/snow mixing ratio, and the cloud water/ice mixing ratio. The model physics include bulk schemes, mixed-phase physics of cloud-resolving modeling, and multi-layer land surface models ranging from a simple thermal model to full vegetation and soil moisture models. The full vegetation and soil moisture land surface models can include snow cover and sea ice, turbulent kinetic energy predictions or non-local K schemes for planetary boundary layer calculations, longwave and shortwave schemes with multiple spectral bands, and a simple shortwave model. On the other hand, the WRF Preprocessing System (WPS) is used to prepare a domain (region of the earth) for WRF. The WPS consists of three independent programs: *geogrid*, *ungrib*, and *metgrid*. The purpose of *geogrid* is to define the simulation domains and interpolate various terrestrial data sets to the model grids. The *ungrib* program reads GRIB files, *degrids* the data, and writes the data in a simple format, called the intermediate format. The *metgrid* program horizontally interpolates the intermediate-format meteorological data that are extracted by the *ungrib* program into the simulation domains defined by the *geogrid* program. A detailed description of the WRF and WPS model can be found on the WRF website [34].

In addition to a dynamical calculation, a chemical model (WRF/Chem) is full (on-line) coupled with the WRF model. A detailed description of WRF/Chem is given by Grell et al. [34]. The version of the model (version 3.3) used in the present study includes simultaneous calculations of dynamical parameters (e.g., wind, temperature, boundary layer, and clouds), transport (advective, convective, and diffusive), dry deposition [35], gas phase chemistry, radiation and photolysis rates [36, 37], and surface emissions, including online calculations of biogenic emissions. Ozone chemistry is represented in the model by a modified Regional Acid Deposition Model version 2 (RADM2) gas-phase chemical mechanisms [38], which includes 158 reactions among 36 species, in conjunction with the Secondary Organic Aerosol Model (MADE/SORGAM) of aqueous reactions [39].

2.2 Model settings and initialization

The WRF/Chem model is adapted to have four nested domains with horizontal resolution of 330 km, 110 km, 36 km and 12 km (Figure 1). The outermost domain covers the coastal areas of the Sea of Japan, which include the main island of Japan (Honshu Island) and adjoining the western Pacific Ocean and the East Sea [40, 41]; the second domain with 110 km resolution covers resolution covers the Greater Tokyo Area, which is a large metropolitan area in Kanto region, Japan, consisting of most of the cities of Chiba, Kanagawa, Saitama, and Tokyo (at the center) and a part of Yamanashi and Ibaraki Prefecture, the adjoining ocean region; the third domain with 36 km covers a part of Tokyo, Kanagawa and Chiba Prefecture and the innermost 12 km domain covers Kawasaki City. Kawasaki is a city located in Kanagawa Prefecture, Japan, between Tokyo and Yokohama. It is the 9th most populated city in Japan and one of the main cities forming the Greater Tokyo Area and Keihin Industrial Area.

In this study, the model was used to simulate medium-scale and regional circulation influenced by the complex terrain within and around the coastal areas of the Sea of Japan during the period from 00:00 UTC (Coordinated Universal Time) [42] on August 14, 2010 to 00:00 on August 18, 2010; Japan Standard Time (JST) [43] is the standard time zone of Japan and is 9 hours ahead of the UTC. A four

nesting domain was defined using the Lambert projection, which can be observed in Figure 1. The domain settings and configuration options are shown in Table 1. The initial and lateral boundary conditions for meteorology component are taken from the National Centers for Environmental Prediction (NCEP) Final (FNL) Global Analysis data available at 1° resolution and at six hour intervals. The ideal concentration profiles [44] were used as initial and boundary conditions of the chemical species. A total of 35 vertical levels with 10 levels in the lower atmospheric region (below 800 mbar) was considered in the model.

In general, models will have spin-up time; that is the time needed to adjust to forcing. In weather prediction, the model physics will spin up a velocity field in balance with the density field, even in the absence of forcing. As forcing is applied, the velocity field will respond to it initially with transient flows that may not be realistic although continuously changing. For this reason, the model simulation was started from 00:00 UTC on 6 August to 00:00 UTC on 18 August, where the first 8 days simulation results were not used in this study. The model is executed with 8 days spin-up to achieve stabilized results of this study.

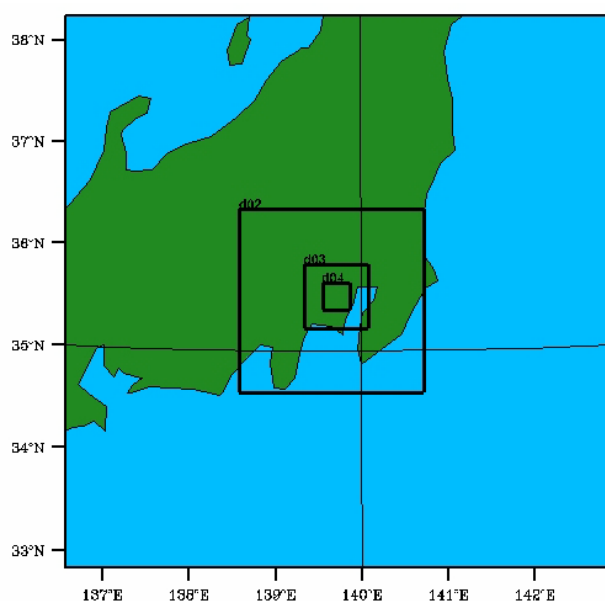


Figure 1. The nesting domain setting of the model

Table 1. WRF/Chem model domain settings and configuration options

Dynamics	Primitive equation, non-hydrostatic			
Vertical resolution	35 levels			
Domains	Domain 1	Domain 2	Domain 3	Domain 4
Horizontal resolution	330 km	110 km	36 km	12 km
Domains of integration	32.8°N-38.3° N; 136.5°E-143° E	32.7°N-36.4° N; 138.6°E-140.7° E	35.25°N-35.8° N; 139.35°E-140° E	35.44°N-35.62° N; 139.58°E-139.82° E
Microphysics	WSM3-class simple ice scheme [48]			
Advection scheme	5th horizontal/3rd vertical [80, 81]			
Longwave radiation	RRTM [52]			
Shortwave radiation	GODDARD [50,51]			
Surface layer	Moni-Obukhov (Janjic Eta) [49]			
Land surface model	NOAH [55]			
Boundary layer	Mellor-Yamada-Janjic TKE [53, 54]			
Cumulus parameterization	Grell-Devenyi ensemble scheme [82]			
Chemistry option	RADM2 [56]			
Dry deposition	Wesley [35]			
Photolysis option	Madronich [57]			
Aerosol option	MADE/SORGAM [39]			

The chemistry is initialized with idealized profiles, with the anthropogenic emissions data taken from the global emission data “prep_chem_sources” described in Section 3.2. The data are interpolated to model grids using the emissions processing program available with WRF/Chem. The biogenic emissions are calculated using the scheme of Guenther et al. [45, 46]. WRF/Chem simulates concurrently the meteorological conditions and chemistry of atmospheric species from emission, through transport and a variety of chemical reactions, to the removal by wet or dry deposition. The Weather Research and Forecasting model [47] serves as a meteorological module for WRF/Chem. In this study, cloud and the precipitation formation process were simulated by the WSM3-class simple ice scheme [48] that allows for mixed phase processes and the coexistence of super cooled water and ice. To consider the impact of cumulus convection, despite convection only occurring on a few days during 14-18 August, the cumulus ensemble approach had been used [49]. Shortwave radiation was determined by the Goddard two stream multi-band schemes [50, 51] and RRTM scheme [52], respectively, that considers, among other things, cloud effects and ice-fog. Long wave radiation was treated with the Rapid Radiative Transfer Model [52], that considers multiple spectral bands, trace gases, and microphysical species. Turbulent processes in the atmospheric boundary layer were determined using the Mellor-Yamada-Janjic TKE scheme [53, 54]. However, the Monin-Obukhov similarity hypotheses were used to describe the turbulent processes in the atmospheric surface layer, where Zilitinkevich’s thermal roughness length concept was considered for the underlying viscous sublayer [54]. The exchange of heat and moisture in the land atmosphere interface was described by the Noah land surface model (NOAH) [55] which calculates soil temperature and moisture states, including frozen soil physics. Its multi-layer snow model and one-layer vegetation model considers snow and vegetation processes, respectively. The chemistry options used in the model are the Regional Acid Deposition Model version 2 (RADM2) gas-phase chemical mechanisms [56] and Madronich photolysis scheme [57]. For the present study, the MADE/SORGAM [39] aerosol module is included. The chemistry was initialized with idealized profiles. The various options used in the model are given in Table 1.

2.3 Emission data acquisition

The use of a global emissions data set has recently been added to the WRF/Chem model options. The global emissions data are from the REanalysis of the TROpospheric (RETRO) chemical composition data collected over the past 40 years and the Emission Database for Global Atmospheric Research (EDGAR). Both RETRO and EDGAR provide global annual emission data of several greenhouse gases (e.g., CO₂, CH₄ and N₂O) as well as some precursor gases on a 0.5°×0.5° (RETRO) or a 1°×1° (EDGAR) grid. In the present study, a simple grid-mapping program was used in the WRF/Chem model. This program, called “prep-chem-sources” for global emission data (dust, sea salt, biomass burning), was developed at CPTEC, Brazil and is available to WRF/Chem model users. The “prep-chem-sources” is an emission data generator package to provide gridded emission fluxes (kg/m²) which assimilates the inventory works (Table 2) of biomass burning and wildfire emission data from anthropogenic and biogenic sources [58].

The GEIA (Global Emissions Inventory Activity)/ACCENT (European Network of Excellence on Atmospheric Composition Change) data portal is a cooperative project that provides surface emission data (total and gridded data) for the main emission categories (total anthropogenic, total biomass burning, biogenic, and oceans) at global or regional scales from several inventories (e.g., RETRO [59], POET [60, 61], EDGAR [62, 63, 64], GFEDv2 [65, 66], CO₂ [67] and GEIA v1 [59]) (Table 2).

Table 2. Global inventories offered by the GEIA/ACCENT data portal

Inventory	Categories	Spatial resolution	Temporal resolution
POET	Anthropogenic biomass burning (natural)	1°×1°	Annual (anthro.), monthly (biom. burn.), monthly (natural)
RETRO	Anthropogenic biomass burning	0.5°×0.5°	Monthly
EDGAR	Anthropogenic biomass burning	1°×1°	Annual
GFED v2	Biomass burning/wildfire emission	1°×1°	Monthly
CO ₂	Anthropogenic	1°×1°	Annual
GEIA v.1	Anthropogenic biomass burning naturally	1°×1°	Annual + monthly for NO _x , SO ₂ , and nat. VOC

2.4 Air quality monitoring

Air quality monitoring data in Tokyo, Kanagawa and Chiba Prefecture operated by Japanese local government are explained in this section. Annual and monthly pollutant concentrations observed at different monitoring stations in Japan are available on the website of the National Institute for Environmental studies [68]. This site contains data that has been collected since 1970, which are valuable for evaluating the long-term or short-term trends of pollutant concentrations in Japan. The observation data set of this section investigates the pattern of ozone concentrations with its precursors (NO, NO₂ and NO_x) to investigate their range in Tokyo, Kanagawa and Chiba Prefecture in 2010. In this study the monitoring data has been compiled from 87 monitoring stations in Tokyo, 92 monitoring stations in Kanagawa and 143 monitoring stations in Chiba. Most of the monitoring stations are located in populated areas in Japan, described by Chatani and Sudo [28], because these stations are operated primarily to ensure adherence to environmental quality standards (EQSs). This database has been compiled from surface pollutant concentrations recorded as daytime and nighttime averages and from the maximum concentrations of photochemical oxidants and other pollutants. Daytime corresponds to a twelve-hour period from 06:00 a.m. to 06:00 p.m. and nighttime corresponds to a twelve-hour period from 06:00 p.m. to 06:00 a.m. of Japan Standard Time. Photochemical oxidants include other trace oxidants such as H₂O₂ and peroxyacyl nitrates (PANs), but instruments that detect only ozone have been officially approved by the Japanese government because differences in concentrations of photochemical oxidants and ozone are expected to be small [28]. Therefore, differences in concentrations between ozone and photochemical oxidants can be ignored for monthly variations in observed surface ozone concentrations.

Figure 2 shows the monthly variation of observed averaged concentrations of ozone, NO, NO₂, and NO_x at the monitoring stations in Tokyo, Kanagawa and Chiba Prefecture from January to December 2010. The average ozone concentrations were found to be the maximum value about 46 ppb around the spring (April to May). It decreased in summer (July) and reached a minimum value about 15 ppb in winter (November to December). The monthly variation of observed ozone concentration above populated Japanese areas averaged over 1996–2008 prepared by Chatani and Sudo [28] shows a clear seasonal variation that is repeated consistently year after year. On the other hand, the monthly average NO concentrations were observed about 4–30 ppb, NO₂ were observed about 10–30 ppb, NO_x were observed about 25–60 ppb over Tokyo, Kanagawa and Chiba Prefecture. The trend of monthly average NO, NO₂ and NO_x concentrations shows that it was lower in spring and summer (April–September), which started increasing in autumn to winter (October to January). The observation data sets has shown that there have been a high ozone episod (monthly average concentration was about 45 ppb) in the month of April to May at most of the monitoring stations in Tokyo, Kanagawa and Chiba Prefecture, in which the concentrations of NO, NO₂, and NO_x were considerably lower. On the other hand month average ozone concentration was lower in winter (November, December and January) about 15–20 ppb, where the concentrations of NO, NO₂, and NO_x were considerably higher.

Figure 3 shows the monthly pick value of ozone, NO and NO₂, which was observed once a month at one of the monitoring stations. In this case the maximum values were selected once a month from all observation data of the monitoring stations of Tokyo, Kanagawa and Chiba Prefecture. The pick value of ozone was observed in August 2010 at one of the monitoring stations of Tokyo Prefecture (155 ppb), Kanagawa Prefecture (168 ppb) and Chiba Prefecture (160 ppb). The Figure 3 shows that the pick values of ozone concentrations were observed in the Greater Tokyo Area at the different monitoring stations in the summer season (August) in 2010. In this paper, a serious and continuous high ozone episode in the Greater Tokyo Area (GTA) during the summer of 14–18 August 2010 was investigated using the observation data. We observed and analyzed the ozone and other trace gas concentrations, as well as the corresponding weather conditions in this high ozone episode by WRF/Chem model. Our aim was to further understand the physical and chemical mechanisms of this high ozone episode by use of the new generation air quality model WRF/Chem.

The Kawasaki City Air Pollution Monitoring Centre (KCAPMC) (35° 31' 52" N, 139° 42' 17"E) gathers environmental data of air and water through an automatic monitoring system, and analyzed environmental data to utilize in the city's environmental administration as well as being simplified and actively provided to the citizens and local businesses. The detail descriptions of the monitoring data as well as the monitoring methods are available in the website of Kawasaki City Air Pollution Monitoring Centre [69]. This site contains hourly time series data of pollutant concentration that has been collected

since 1979, which are valued from 1996 for evaluating the yearly trends of pollutant concentrations in this city. Figure 4 shows the geographical location of Kawasaki City.

Figure 5 plots long-term yearly variations in ozone, NO, NO₂, NO_x concentration measured by KCAPMC in the period from 1979 to 2010. The time series of ozone show regular shorter changes with long-term trends. However, some exceptions can be seen. The average annual concentration of ozone in the baseline year (1979) was 15 ppb. In 2010, the average annual concentration was 30 ppb, an increase of 100 percent. The general trend shows that there has been a steady increase in average annual ozone concentration between 1979 and 2010. Annual variations are due primarily to variations in weather conditions, which can have a significant impact on ground-level ozone formation. Figure 2 shows that ozone concentration is lower in winter season and higher in spring. Due to the global warming, the winters of the present decade are warmer and dryer than other previous decades, caused higher ozone concentration from 2004 in Kawasaki City. In addition, the yearly average concentrations of NO, NO₂, NO_x in Kawasaki City were higher from 1984 to 1992 and gradually decreased every year till 2010.

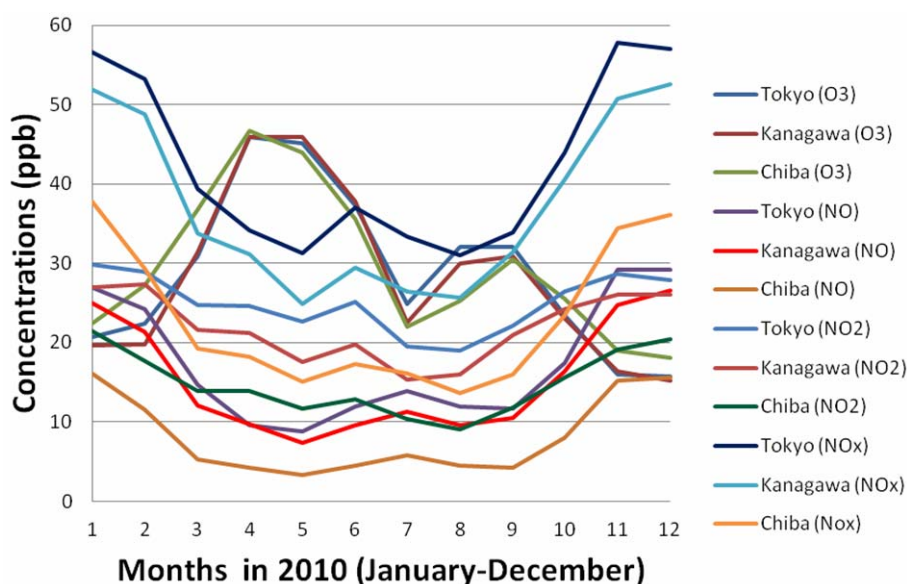


Figure 2. Monthly variation of observed ozone, NO, NO₂, and NO_x concentrations at the monitoring stations of Tokyo, Kanagawa and Chiba Prefecture from January to December 2010

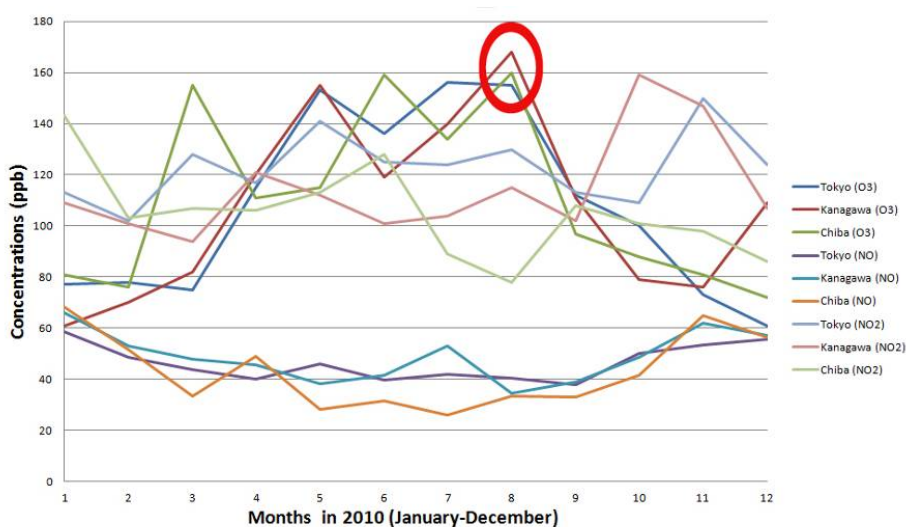


Figure 3. The monthly pick value of ozone, NO and NO₂, which was observed once a month at one of the monitoring stations in Tokyo, Kawasaki and Chiba Prefecture. The red circle shows the pick value of ozone in 2010



Figure 4. The geographical location of Kawasaki city air pollution monitoring centre ($35^{\circ} 31' 52''$ N, $139^{\circ} 42' 17''$ E)

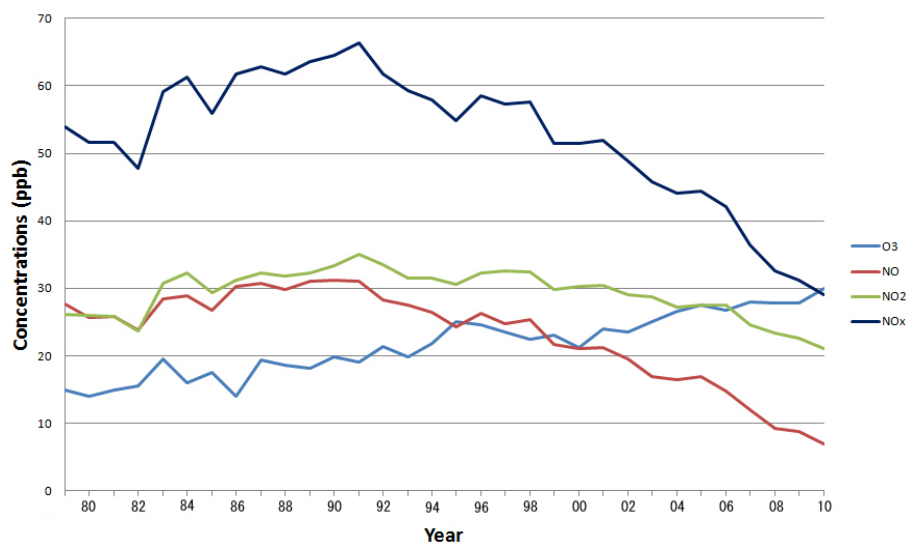


Figure 5. Yearly variations of observed ozone, NO, NO₂, NO_x concentrations, averaged over 1980-2010 in Kawasaki City

Since the pick ozone concentrations were observed in October in the Greater Tokyo Area of Japan, an attempt has been taken to examine the evolution of surface ozone from 14 to 18 October 2010 by WRF/Chem simulation. The highest ozone concentration occurred from 14 to 18 October 2010 in Kawasaki City, lasting for 3-4 days, which can be expressed as a high ozone episode. Prior to this high ozone episode, the surface ozone concentrations were low on 13 October (about 40–80 ppb) and reached to 100 ppb at 12 p.m. on 14 October (JST). The red circle in Figure 6 shows the peak higher value of ozone concentration was identified about 168 ppb at 12 p.m. (JST) on October 15. The peak higher value of ozone concentration could be called an high ozone episode (Figure 6). The second higher pick value was found about 162 ppb at 12 p.m. (JST) on October 16. The range of ozone concentration in October 2010 in Kawasaki City was observed about 3.2 – 168.8 ppb, where the average ozone concentration was 32 ppb. Figure 6 shows time series (3 hours interval) ozone, NO, NO₂, NO_x concentrations from 00:00 a.m. on 1 August to 00:00 p.m. on 31 August (JST) of 2010. The range of NO₂ concentrations in October 2010 in Kawasaki City was 6-43 ppb with an average value of 18 ppb. Similarly, the range of NO concentrations was 0-32 ppb with an average value of 7.5 ppb and the range of NO_x concentrations was 7-63 ppb with an average value of 25 ppb.

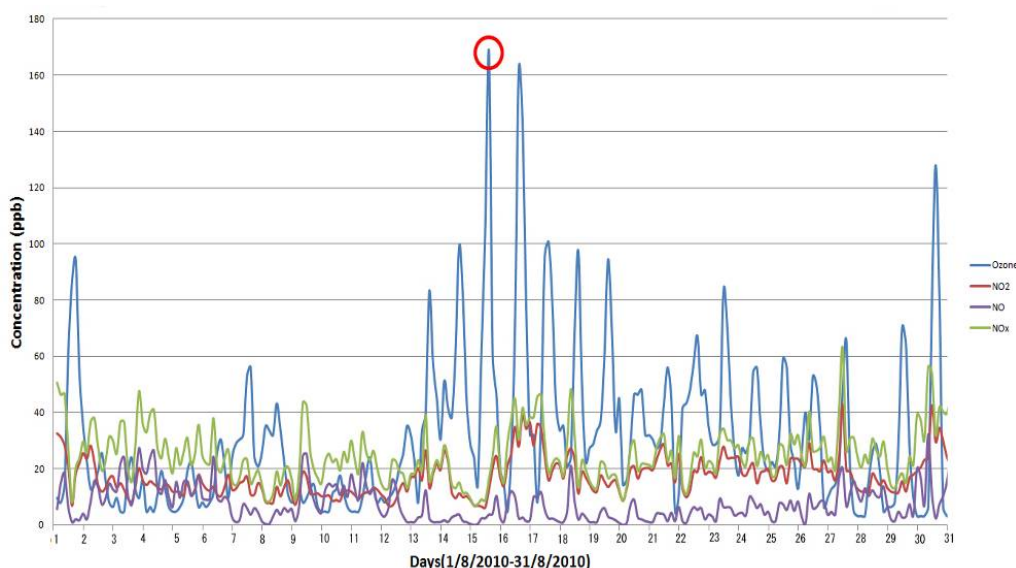


Figure 6. Time series (3 hours interval) ozone, NO, NO₂ and NO_x concentrations from 00:00 a.m. on 1 October to 00:00 p.m. on 31 October of 2010 (JST) at Kawasaki City. The red circle shows the peak ozone concentration (168 ppb) at 12 p.m. on 15 October (JST), which could be called an ozone pollution episode

3. Results and discussions

3.1 Model evaluation

The model results were evaluated by the time series of ozone concentrations measured in KCAPMC. However, meteorological measurements by AMeDAS (Automated Meteorological Data Acquisition System) [70] from 20 meteorological stations in Tokyo Prefecture, 18 meteorological stations in Chiba Prefecture and 11 meteorological stations in Kanagawa Prefecture were also compared with WRF/Chem simulation results. Basic statistics (mean error, ME; mean absolute error, MAE; root mean square error, RMSE) are shown in Table 3 for ground level temperature, wind speed. Evaluation of surface temperatures revealed good agreement for simulated daytime temperatures, while nighttime cooling was systematically underestimated, resulting in better outcomes for hourly values than for daily maxima statistical scores (Table 3). Due to predominating weak meso-scale air motions during the summer season in Japan, it was difficult to accurately simulate the winds. Fairly good agreement between the model and measurements was obtained for winds speed and direction at Chiba Prefecture meteorological stations, with more pronounced and consistent circulations (land-sea breezes coupled with up- and down-slope coastal winds). The ranges of ground level temperatures in GTA were observed 28-38°C at daytime and 22-33°C nighttime during the simulation period. In August, ground level wind speed is usually lower in Japan. The average wind speed was observed about 2.7 m s⁻¹ in GTA, where the nighttime wind speed was almost calm about 1-2 m s⁻¹ and daytime wind speed was slightly higher 3-4 m s⁻¹ during the simulation period. Water vapor mixing ratios were calculated about 4-26 g/kg by the WRF/Chem during the simulation period, whereas the observation data of water vapor mixing ratios are not available for GTA in 2010 AMeDAS database.

Table 3. Statistical scores for near-ground temperature (T), wind speed (v), calculated for all hourly values from 49 measuring sites during the simulation period. In the case of temperature, daily maxima (index max) are also analyzed

	T _{max} (°C)	T (°C)	v (m s ⁻¹)
ME	0.72	1.8	1.2
MAE	2.1	2.5	1.4
RMSE	2.6	3.1	2.2

Figure 7 and Figure 8 compare measured and simulated values of ozone, NO, NO₂ and NO_x during the high ozone episode at Kawasaki city air quality measurement sites. It can be seen that the model

performs better to simulate the concentration of ozone in Kawasaki city than that of its precursor (NO, NO₂ and NO_x). In the monitoring station's nighttime ozone values were slightly overestimated and daytime ozone was underestimated by the model. Most pronounced is the nighttime ozone overestimation at the Kawasaki city, with significantly low measured nighttime ozone values. Low measured nighttime ozone values, otherwise usually common for populating urbanized areas, can in the case of this site be explained by the formation of an unstable nighttime boundary layer above the glade (where the site is located) surrounded by mountains and buildings. At nighttime, the presence of the nocturnal inversion layer isolates the ground-level ozone from that of the upper levels. Surface ozone is removed by deposition and titration with nitric oxide (NO) from evening traffic and industrial emissions. Since no ozone is produced in the absence of sunlight at night, ozone concentration decreases after sunset [71]. Therefore, sometimes NO_x, NO₂ and NO concentrations were found higher in nighttime in this area. Basic statistics (ME, MAE, RMSE) are shown in Table 4 for ground level concentrations of ozone, NO_x, NO₂ and NO. Evaluation of surface concentrations of ozone, NO_x, NO₂ exposed a reasonable agreement with WRF/Chem simulation in Figure 6 and Figure 7 but the performance of WRF/Chem was not so reasonable for the simulation of NO concentration during the simulation period. Figure 7 shows hourly average concentrations of ozone, NO_x, NO₂ and NO at KCAPMC sites during the simulation period. The ozone concentrations were relatively low at night time (about 16–62 ppb), it rose during daytime and reached the highest ozone concentration (about 36-110 ppb). Figure 7 gives the hourly average concentrations of ozone observed at the KCAPMC site compared with WRF/Chem simulation. Looking at the highest and lowest value of ozone, NO_x, NO₂ and NO at the KCAPMC site, some overestimation and underestimations can be noted, where the agreement varies between high ozone episod and measuring sites as well (Figure 7 and Figure 8). Ozone daily maxima, which are of most concern, are generally not simulated at the exact times and exact locations of the measurements. To exclude the influence of model time lag (ozone peaks simulated well, but not at the exact time), a scatter plot for the value of ozone, NO_x, NO₂ and NO regardless of the time of occurrence is added in Figure 8.

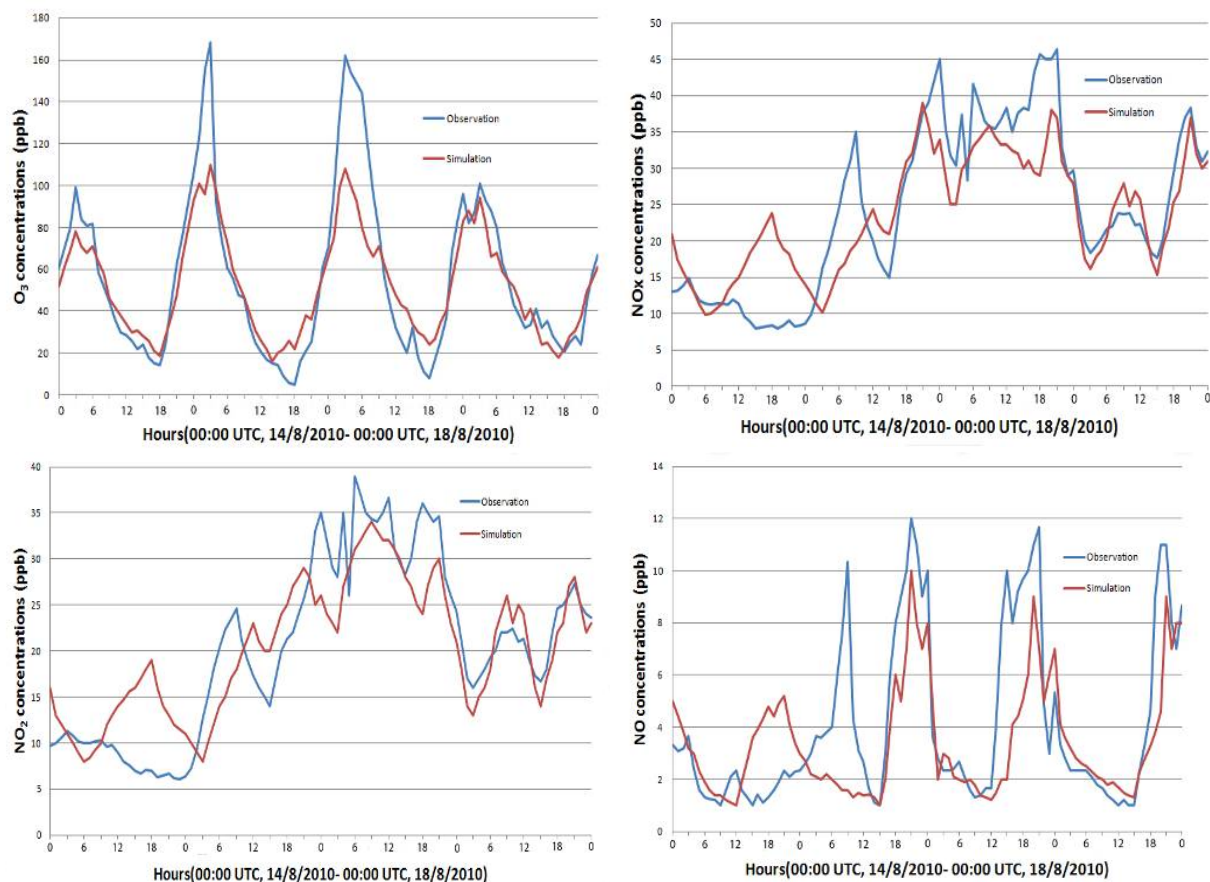


Figure 7. Time series of simulated (blue lines) and measured (red lines) ozone, NO, NO₂ and NO_x values at KCAPMC during the simulation period

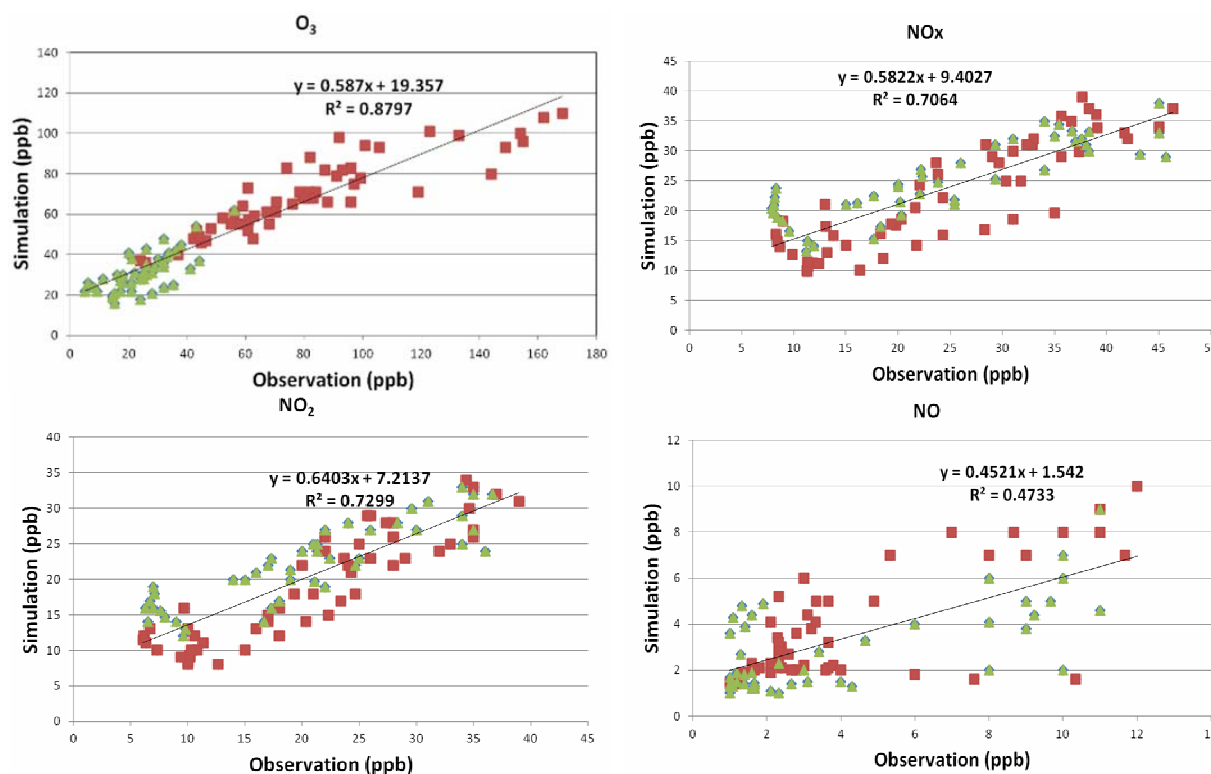


Figure 8. Scatter plots of simulated and measured hourly values of ozone, NO_x, NO₂ and NO at KCAPMC during the simulation period. Red dots represent daytime hours (6-18UTC), while Pale green triangles represent nighttime hours

As shown in Figure 8, an excellent correlation was found between the simulated and measured hourly values of ozone, NO_x, NO₂ and NO at KCAPMC during the simulation period. The correlation coefficient R was 0.88 for the simulated and measured hourly values of ozone and the regression line passes near the origin, where the variance can be explained by different reasons. Underestimations of ozone concentrations can be related to local effects not sufficiently resolved by the model at the monitoring station. Another reason could be the simulated PBL height, which tended to be underestimated in the simulations. Very high PBL heights (up to 2.5 km) were simulated during the simulation period. This could explain daytime ozone underestimations at the KCAPMC site during the simulation period, due to excessive daytime mixing leading to too-efficient dilution of the pollutants. Similarly, PBL heights up to 2.5 km were simulated during the daytime of the advection phase of the simulation period over Kawasaki City areas, which could again contribute to underestimate ozone levels at the observation site. The correlation coefficient R was 0.70, 0.72 and 0.47 for the simulated and measured hourly values of NO_x, NO₂ and NO respectively. In this case the value of NO calculated by the WRF/Chem model was underestimated most of the time during the simulation period at the monitoring site, where the variances were caused by the dilution of NO by the effect of higher PBL. The hourly values of NO₂ concentrations were overestimated by the WRF/Chem model at daytime because a greater proportion of the NO is oxidized to NO₂, resulting in a greater amount of ozone formation [$O_3 + NO \rightarrow NO_2 + O_2$]. Moreover, the discrepancy of simulation and observation value of NO₂ and NO_x mainly occurred due to the coarse resolution of emission inventory, where the primary sources of NO_x production are combustion processes, including industrial and electric generation processes, and mobile sources such as automobiles [72].

3.2 Characteristics of high ozone episode

During the four day simulation period, it was found that the higher ozone concentrations were found in the daytime (12-15 JST) and lower ozone concentrations were calculated in the nighttime. The model calculated the maximum ozone concentration in 12 JST of 15 August, which was about 110 ppb (Figure 9). Figure 9 shows the daytime and nighttime ozone concentration (ppb) at the Kawasaki City for the finest domain (Domain 4) with 12 km resolution during the simulation period.

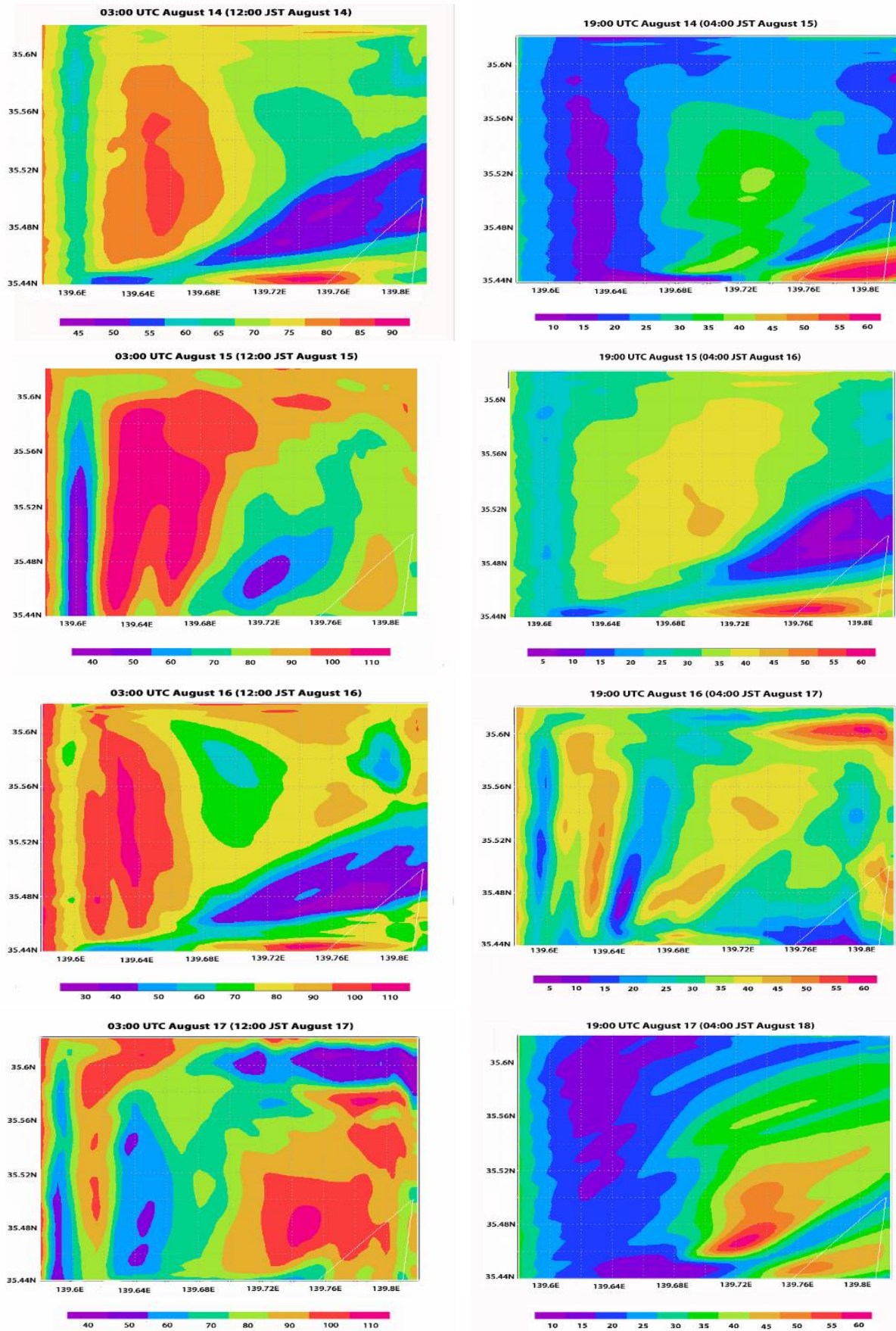


Figure 9. Daytime and nighttime ozone concentration (ppb) at Kawasaki City for the finest domain (Domain 4) with 12 km resolution during the simulation period

Table 4. Statistical scores for near-ground level concentration of O₃, NO_x, NO₂, NO calculated for all hourly values from KCAPMC sites during the simulation period

	O ₃ (ppb)		NO _x (ppb)		NO ₂ (ppb)		NO (ppb)	
	Daytime	Nighttime	Daytime	Nighttime	Daytime	Nighttime	Daytime	Nighttime
ME	12.51	6.48	2.06	0.7	1.69	1.81	0.37	1.1
MAE	16.33	8.58	4.29	5.76	3.6	4.54	1.37	2.12
RMSE	23.57	10	5.69	7.26	4.39	5.6	2.08	6.4

Summer ozone [1] episode over Japan are usually characterized by high temperatures and air masses recirculating over the coastal area of Japan due to the effect of sea and land bridge. These conditions typically result in summer smog episodes as the ozone precursor chemicals react in the presence of sunlight. The August 2010 high ozone episode can be characterized by these two factors. It is important that both high temperatures and re-circulation of air masses are coupled together to result in a summer smog episode. In the model, a weak flow around the Kawasaki City may have occurred at the lowest model levels, but in general in the planetary boundary layer the local meso-scale winds developed and governed the pollutant transport and dispersion. The Kawasaki City was in this phase of the episode included in the wider air circulation over the coastal area of the Sea of Japan. Its coastal regions were under the combined coastal sea/land breezes and up-slope/down-slope air circulations of the mountainous area, which contributed to significantly higher ozone mixing ratios measured at the KCAPMC site during this phase. The good agreement between higher temperature and higher value of water vapor mixing ratio over the Sea of Japan coastal area (Figure 10 and Figure 11), led to higher daytime ozone concentration shown in Figure 9. Figure 10 shows daytime value of water vapor mixing ratio (g/kg) at Kawasaki City over the finest domain (Domain 4) with 12 km resolution during the simulation period. The adsorption of the outgoing solar radiation at daytime by the water vapor in the air causes the formation higher ozone concentration on the ground level, whereas the vertical profile of the of water vapor mixing ratio shows a higher value on the ground level [73]. Figure 10 shows the highest value of water vapor mixing ratio during the episode, which was about 24-26 g/kg. Therefore, higher value of water vapor mixing ratio can be treated as an ozone precursor. Meanwhile, the strong sunlight and hot weather cause ground level ozone to form in harmful concentrations in the air, which is mainly a daytime problem during the summer months. Figure 11 shows the daytime value of air temperature (°C) at Kawasaki City over the finest domain. The daytime value of air temperature on the ground level was simulated about 30-38 °C by the WRF/Chem model during the episode.

3.3 Atmospheric NO_x concentrations

NO_x (NO+NO₂) is directly emitted from surface sources, which can be transported 1 days to 1 week. Its chemical lifetime on the surface is about 1-2 days [74], so that NO, NO₂ and NO_x distributions are determined by a combination of chemistry, transport and emission processes. Figure 12 shows the calculated surface NO₂ distribution, with maximum concentrations in early morning (06:00 JST) and early evening (18:00 JST) over the Kawasaki City. It should be mentioned that a minor correlation between the concentrations of NO and NO₂ was observed in this city during the simulation period (Figure 13). Since Kawasaki is an urbanized and industrially developed metropolitan city in Japan, NO₂ and NO usually emitted from automobiles and industrial sources. Roadside emissions of NO₂ and NO usually occur from 06:00 JST to midnight and industrial point source emissions occur 24 hours in this city. Figure 13 depicts a correlation between NO₂ and NO concentrations at KCAPMC during the simulation period, where the regression line passes near the origin and the correlation coefficient R was calculated 0.25. This correlation proves that this area is highly influenced by the local anthropogenic emissions of NO and NO₂, where the variance can be explained by the atmospheric chemical reactions of NO for ozone formation. NO_x concentrations fall significantly due to both an increase in vertical mixing as the PBL deepens, and a noontime maximum in chemical loss by reaction with OH and organic radicals (i.e., OH + NO₂ + M → HNO₃ + M) (Figure 7). NO_x concentrations rise again in the evening, as the PBL height decreases, then, as in the case of CO, transport by down-slope mountain winds moves nighttime NO_x levels in a very narrow area in the center of the city (figure not shown). Changing NO_x emissions has a very different effect on ozone concentrations [75]. In fact, both increases and decreases in NO_x concentrations lead to decreases in ozone concentrations. This implies that the concentration level of NO_x in KCAPMC was at a threshold point producing maximum ozone concentrations during the

episode. At night, changes in NO_x concentrations have large impacts on ozone concentration. Increasing NO_x concentrations reduces early nighttime ozone concentrations, while decreasing NO_x emissions leads to higher nighttime ozone (figure not shown).

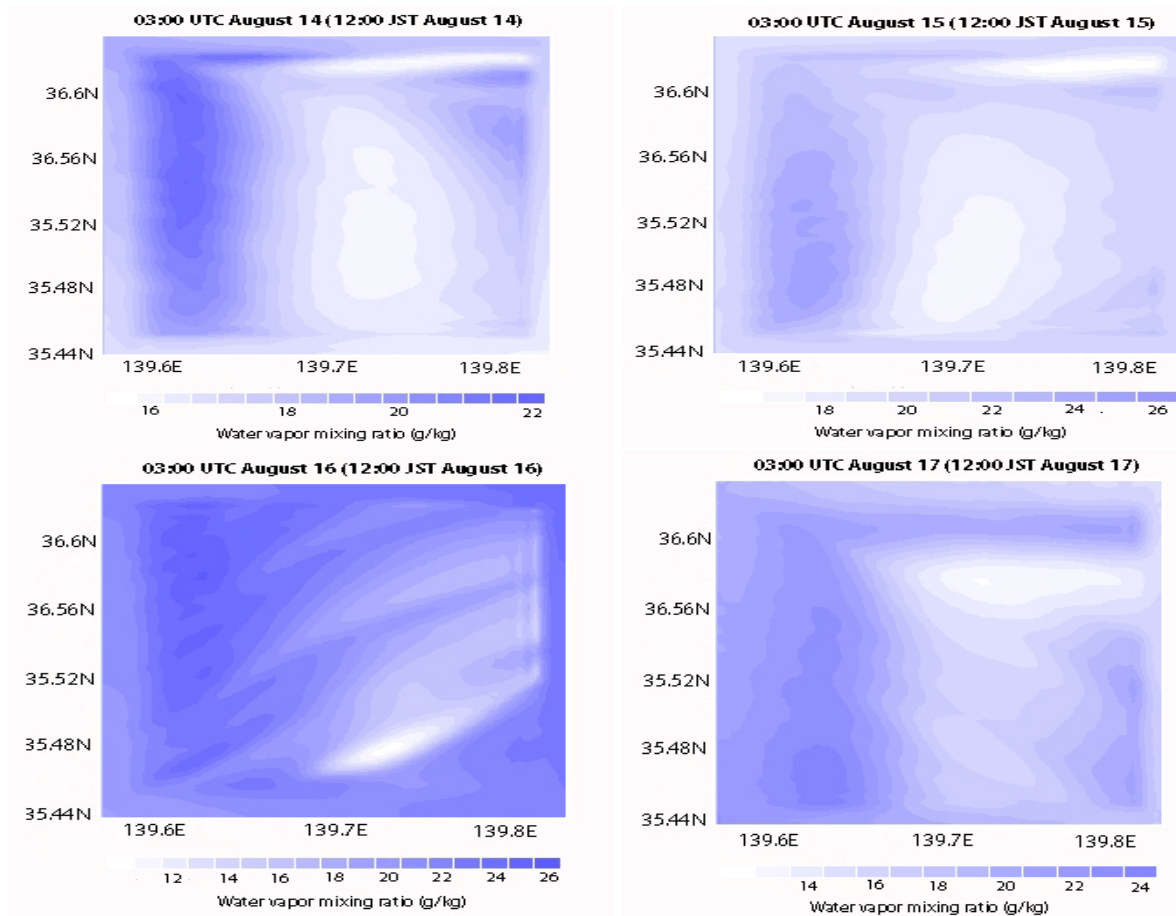


Figure 10. Daytime value of water vapor mixing ratio (g/kg) at Kawasaki City over the finest domain (Domain 4) with 12 km resolution during the simulation period

3.4 Cause of high ozone formation

Polluted air masses were transported from the sea areas near the Tokyo Bay (18:00 UTC August 14, Figure 12) to coastal areas and dispersed over the inland areas, where these air masses remained photochemically active with high ozone levels during daytime and nighttime hours. In the high ozone episode (03:00 UTC August 15), analyses of model results showed that the maximum of the total ozone mass in the lower 2 km of the atmosphere often remained over the coastal areas during daytime hours, while during the night the total ozone mass in the same atmosphere layer was higher over the sea. On the next day of the episode (03:00 UTC August 16) the ozone rich layer started to build up over the Kawasaki City, while from 14 August onwards ozone pollution was spread over the GTA, with the maximum total ozone mass (in the lower 2 km of the atmosphere) over the east coasts, indicating the influence of Tokyo Bay pollution. The role of the coastal pollution reservoir in the Kawasaki City coastal ozone levels during the accumulation phase and the GTA ozone levels during the advection phase was particularly important in this episode. The ozone maximum was also formed in the next day (03:00 UTC August 16) of the accumulation phase of the episode, although the accumulation phase was rather short for this episode and the advection of sea areas near Tokyo Bay polluted air masses contributed to the ozone maximum over the GTA (Figure 12).

The phenomena which contributed to the formation of the ozone rich layer were related to regional scale flow characteristics and meso-scale circulations. The sea areas near Tokyo Bay acts as a pool, where air masses may persist and pollutants advected from more distant areas can accumulate. In addition, during the accumulation phase, the characteristic diurnal cycles of meso-scale flow regimes develop and

contribute to effective injection of coastal emissions and formation of lifting pollutant layers. These diurnal meso-scale flow regimes consist of morning sea-breeze developed in the coastal area of the sea, subsequent coupling of sea-breezes and land-breeze. Similar processes have been observed enabling the formation and transport of pollutant layers, for example in Athens [76], Los Angeles [77], and over the northern [78] and eastern [79] coasts of Spain.

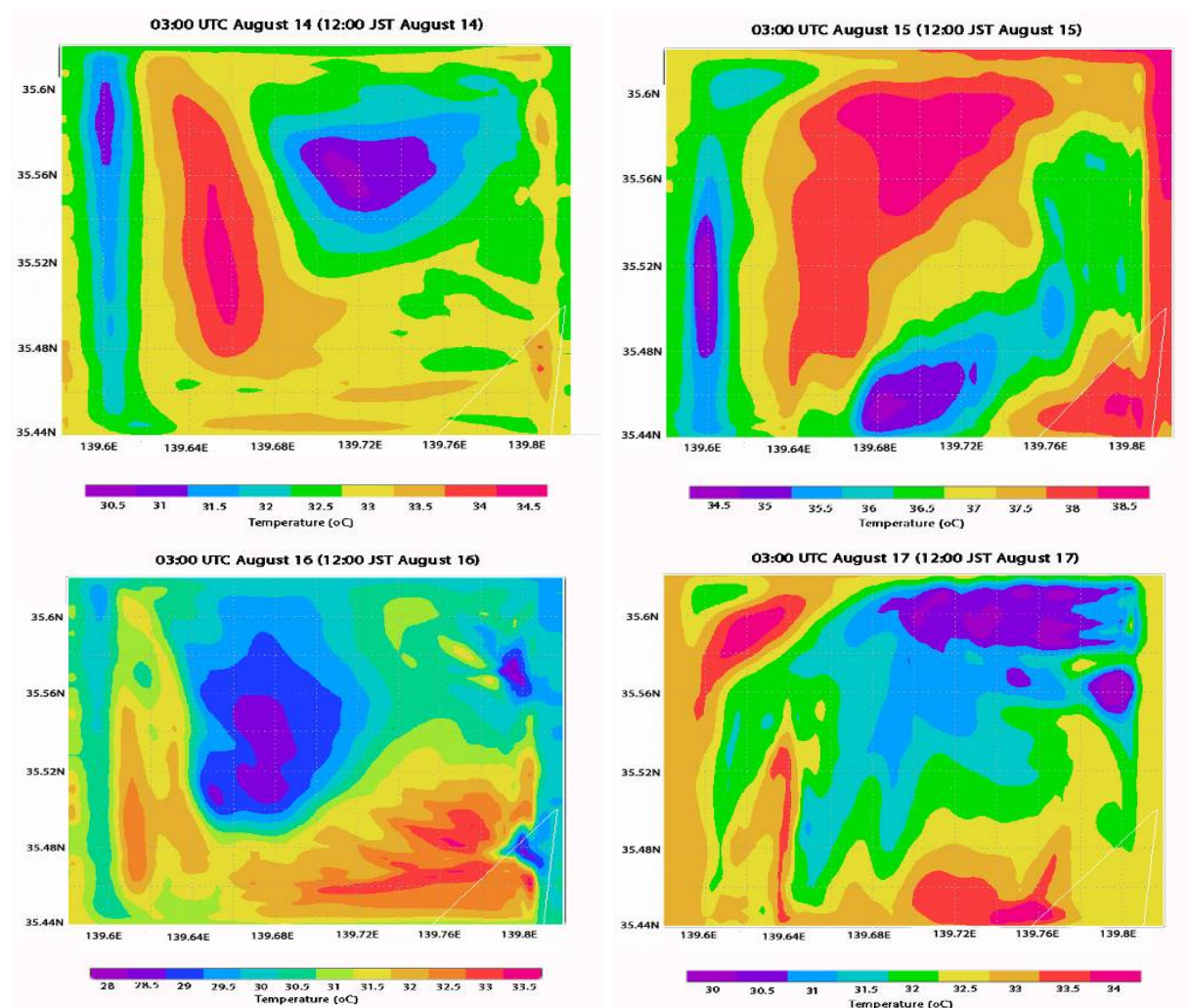


Figure 11. Daytime value of air temperature ($^{\circ}\text{C}$) at Kawasaki City over the finest domain (Domain 4) with 12 km resolution during the simulation period

3.5 The rate of change of ozone concentrations

In order to investigate the chemical characteristics of this continuous high ozone episode, the net production rate of surface ozone was calculated since it can reflect the strength of photochemical reactions to a certain extent. Figure 14 shows the net production rate of surface ozone at KCAPMC. It is obvious that net ozone was produced at day and net lost at night. The production rate reaches its maximum at about 03:00 UTC August 16 (in both observation and simulation), showing that the atmospheric chemical reactions are relatively strong at afternoon, while the greatest loss occurred at about 08:00 UTC August 16 by the observation and 7:00 UTC August 17 by the simulation. On the high ozone episode days (14-18 August), the production and loss of ozone are much more significant, with the highest production rate of 36 ppb h^{-1} by the observation and 24 ppb h^{-1} by the simulation (at 03:00 UTC August 16). However, the maximum loss rate of ozone loss was found 25 ppb h^{-1} by the observation (at 08:00 UTC August) and 16 ppb h^{-1} by the simulation (at 7:00 UTC August 17), respectively. Due to the sufficient ozone precursors and the advantaged weather conditions, ozone can be strongly generated and consumed.

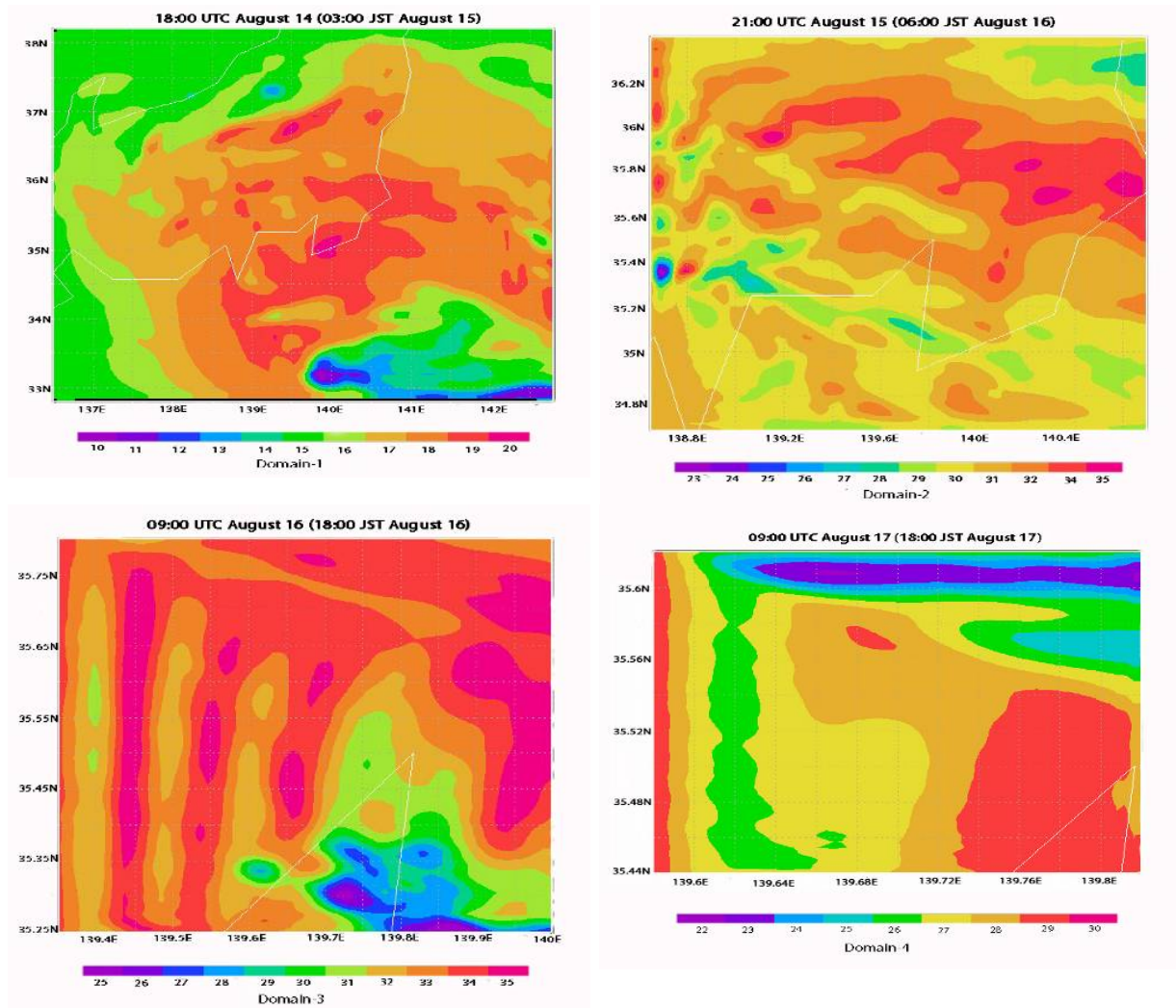


Figure 12. Concentration distribution (ppb) of NO₂ over Domain 1,2,3 and 4

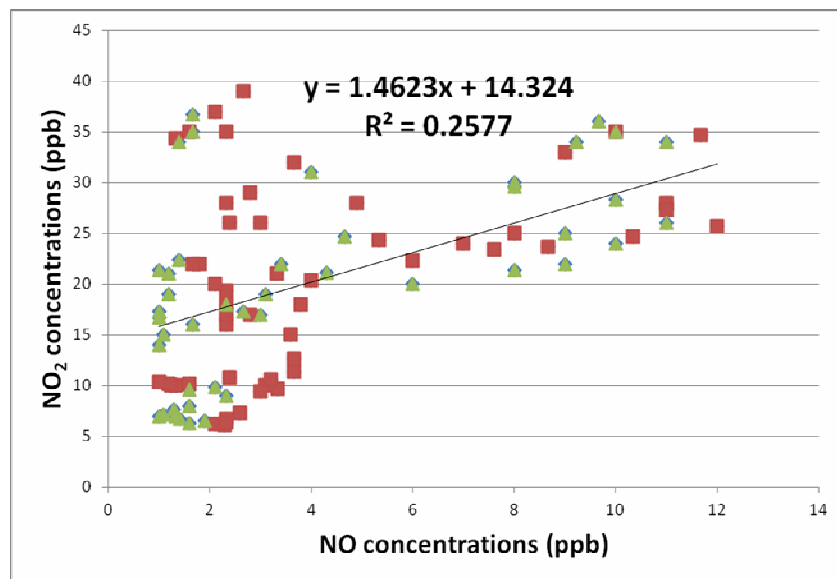


Figure 13. Scatter plots of NO₂ and NO concentrations by observation at KCAPMC during the simulation period. Red dots represent daytime hours (6-18UTC), while Pale green triangles represent nighttime hours

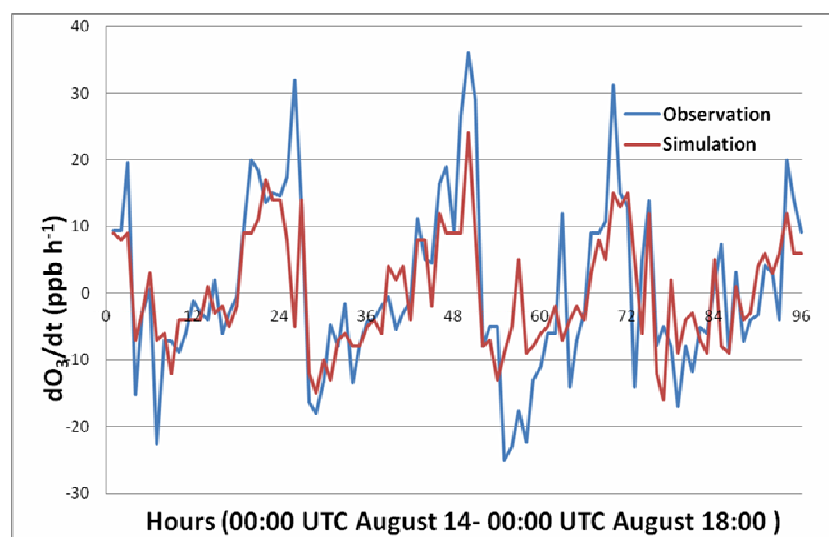


Figure 14. The change rate of surface ozone concentration at KCAPMC

4. Conclusions

By using the new generation of regional air quality model WRF/Chem V3.3, a four-day high ozone episode in the Kanto region (GTA) within 14-18 August, 2010 was investigated. The model represents the diurnal variation of meteorological parameters having a reasonable agreement with observed data, daytime ozone concentrations calculated by the WRF/Chem model was slightly underestimated. Overall, the timing and amplitudes of the calculated diurnal variations of NO₂, NO_x and ozone agreed well with measurements at KCAPMC sites, especially for ozone. The main results and conclusions are summarized as follows. The development of this episode was closely related to the flow of air mass from the sea area as well as the higher value of ground level air temperature and water vapor mixing ratio. The calculated mass flux shows that the horizontal transport by sea breeze and land breeze has strong impact on the surface ozone in the study region. The meteorological conditions induced by the pollutant transport system, such as high temperature, high humidity, weakest outgoing solar radiation also had significant influence on the formation of this continuous episode. The horizontal transport of ozone and its precursors are obvious during this episode. However, it was also responsible for accumulation of ozone in the Kawasaki City. In this high ozone episode, atmospheric chemical processes played an important role in this summer season, the formation and depletion of ozone were much more significant. The largest production rate was found to be about 25 ppb h⁻¹ at the daytime, while the maximal depletion rate was about 16 ppb h⁻¹ at night by the WRF/Chem simulation. WRF/Chem has shown relatively good performance in modeling of this episode, the simulated and the observed ozone concentrations is basically in agreement at KCAPMC, with best correlation coefficients of 0.87. Therefore, it can be served as a powerful tool for air quality prediction in the future for Japan domain.

References

- [1] H. Berkhout, "NRT ozone data and potential use for summer ozone reporting. 12th Eionet Workshop on Air Quality Management and Assessment," European Topic Centre on Air and Climate Change, Limasol, Cyprus, 15-16 October, 2007.
- [2] L. I. Kleinman, P. H. Daum, D. G. Imre, J. H. Lee, Y. N. Lee, L. J. Nunnermacker, S. R. Springston, J. Weinstein-Lloyd and L. Newman, "Ozone production in the New York City urban plume," *Journal of Geophysical Research*, Vol. 105, 2000, pp. 14495–14512. doi:10.1029/2000JD900011.
- [3] L. I. Kleinman, P. H. Daum, Y. N. Lee, L. J. Nunnermacker, S. R. Springston, J. Weinstein-Lloyd, P. Hyde, P. Doskey, J. Rudolph, J. Fast and C. Berkowitz, "Photochemical age determinations in the Phoenix Metropolitan area." *Journal of Geophysical Research*, Vol. 108, 2003, NO. D3, 4096, doi:10.1029/2002JD002621.
- [4] A. Thielmann, A. S. H. Prevot, J. Staehelin, "Sensitivity of ozone production derived from field measurements in the Italian Pobasin," *Journal of Geophysical Research*, Vol. 107, 2002, pp. 8194-8203.

- [5] R. A. Zaveri, C. M. Berkowitz, L. I. Kleinman, S. R. Springston, P. V. Doskey, W. A. Lonneman, C. W. Spicer, "Ozone production efficiency and NO_x depletion in an urban plume: interpretation of field observations and implications for evaluating O₃, NO_x, VOC sensitivity," *Journal of Geophysical Research*, Vol. 108, 2003, NO. D14, 4436, doi:10.1029/2002JD003144.
- [6] S. Wakamatsu and L. S. "Kenneth, A study using a three dimensional photo-chemical smog formation model under conditions of complex flow: Application of the Urban Airshed Model to the Tokyo Metropolitan Area," EPA Project Summary, 1991, EPA/600/S3-91/015 May.
- [7] X. Tie, G. Brasseur, C. Zhao, C. Granier, S. Massie, Y. Qin, P. C. Wang, G. L. Wang and P. C. Yang, "Chemical characterization of air pollution in eastern China and the eastern United States." *Atmospheric Environment*, Vol. 40, 2006, pp. 2607–2625.
- [8] F. H. Geng, C. S. Zhao, X. Tang, G. L. Lu and X. Tie, "Analysis of ozone and VOCs measured in Shanghai: a case study," *Atmospheric Environment*, Vol. 41, 2007, pp. 989–1001.
- [9] X. J. Deng, X. Tie, D. Wu, X. J. Zhou, H. B. Tan, F. Li and C. Jiang, "Long-term trend of visibility and its characterizations in the Pearl River Delta Region (PRD), China," *Atmospheric Environment* Vol. 42 (7), 2008, pp. 1424–1435.
- [10] Q. Zhang, C. Zhao, X. Tie, Q. Wei, G. Li and C. Li, "Characterizations of aerosols over the Beijing region: a case study of aircraft measurements," *Atmospheric Environment*, Vol. 40, 2006, pp. 4513–4527.
- [11] S. Sillman, "The use of NO_y, H₂O₂, and HNO₃ as indicators for ozone–NO_x–hydrocarbon sensitivity in urban locations," *Journal of Geophysical Research*, Vol. 100, 1995, pp. 14175–14188.
- [12] W. Lei, B. De Foy, M. Zavala, R. Volkamer and L. T. Molina, "Characterizing ozone production in the Mexico City Metropolitan area, a case study using a chemical transport model," *Atmospheric Chemistry and Physics*, Vol. 7, 2007, pp. 1347–1366.
- [13] R. Zhang, W. Lei, X. Tie and P. Hess, "Industrial emissions cause extreme diurnal urban ozone variability, Proceedings of National Academy Science, USA, Vol. 101, 2004, pp. 6346–6350.
- [14] M. Zavala, W. Lei, M. J. Molina and L. T. Molina, "Modeled and observed ozone sensitivity to mobile-source emissions in Mexico City," *Atmospheric Chemistry and Physics*, Vol. 9, 2009, pp. 39–55.
- [15] F. H. Geng, Z. Qiang, X. Tie, M. Huang, X. Ma, Z. Deng, J. Quan and C. Zhao, "Aircraft measurements of O₃, NO_x, CO, VOCs, and SO₂ in the Yangtze River Delta region," *Atmospheric Environment*, Vol. 43, 2009, pp. 584–593.
- [16] S. Stephens, S. Madronich, F. Wu, J. B. Olson, R. Ramos, A. Retama, and R. Munoz, "Weekly patterns of Mexico City's surface concentrations of CO, NO_x, PM₁₀ and O₃ during 1986–2007," *Atmospheric Environment*, Vol. 8, 2008, pp. 5313–5325.
- [17] Z. M. Ying, X. Tie, G. H. Li, "Sensitivity of ozone concentrations to diurnal variations of surface emissions in Mexico City: a WRF/Chem modeling study," *Atmospheric Environment*, Vol. 43, 2009, pp. 851–859.
- [18] M. Kida, "Countermeasures on chemical substances in Japan by Air Pollution Control Law," Air Quality Management Division, Environmental Bureau, Ministry of the Environment, Japan, 2005. Available from: (http://infofile.pcd.go.th/air/VOC_kida.pdf?CFID=1412050&CFTOKEN=60317530).
- [19] UNSD (United Nations Statistics Division): Standard Country and Area Codes Classifications. Retrieved 16 July, 2010. Available from: (<http://unstats.un.org/unsd/methods/m49/m49regin.htm#asia>).
- [20] Z. Boybeyi and S. Raman, "Numerical Investigation of Possible Role of Local Meteorology in Bhopal Gas Accident," *Atmospheric Environment*, Vol. 29 (4), 1995, pp. 479–496.
- [21] R. A. Pielke, R. T. McNider, M. D. Moran and D. A. Moon, R. A. Stocker, R. L. Walko and M. Uliasz, "Regional and mesoscale meteorological modeling as applied to air quality studies," *Air Pollution Modeling and Its Application*, VII, Van Dop, H, Steyn, DG, Eds, Plenum Press, New York, 1991, pp. 259–290.
- [22] R. A. Pielke, R. T. McNider, M. Segal and Y. Mahrer, "The use of a mesoscale numerical model for evaluations of pollutant transport and diffusion in coastal regions and over irregular terrain," *Bulletin of American Meteorological Society*, Vol. 64, 1983, pp. 243–249.

- [23] H. Jin and S. Raman, "Dispersion of an elevated release in a coastal region," *Journal of Applied Meteorology*, Vol. 35, 1996, pp. 1611-1624.
- [24] V. Kotroni, G. Kallos, K. Lagouvardos, M. Varinou and R. Walko, "Numerical simulations of the meteorological and dispersion conditions during an air pollution episode over Athens, Greece," *Journal of Applied Meteorology*, Vol. 38, 1999, pp. 432-447.
- [25] R. Lu and R. P. Turco, "Air Pollutant transport in a coastal environment II. Three-dimensional simulations over Los Angeles Basin," *Atmospheric Environment*, Vol. 29, 1995, pp. 1499-1518.
- [26] P. Monti and G. Leuzzi, "A numerical study of mesoscale airflow and dispersion over coastal complex terrain," *International Journal of Environment and Pollution*, Vol. 25 (1), 2005, pp. 239-250.
- [27] M. Uliasz, "The Atmospheric Mesoscale Dispersion Modeling System," *Journal of Applied Meteorology*, Vol. 32, 1993, pp. 139-149.
- [28] S. Chatani, and K. Sudo, "Influences of the variation in inflow to East Asia on surface ozone over Japan during 1996–2005" *Atmospheric Chemistry and Physics*, Vol. 11, 2011, 8745–8758.
- [29] N. Masanori, T. Masayuki, A. Hajime, N. Masahisa, N. Tomohiro, S. Tetsu, M. Yuzo, "Evaluation of vertical ozone profiles simulated by WRF/Chem using lidar-observed data," *SOLA 3*, Vol. 2007, pp. 133–136.
- [30] J. Kurokawa, T. Ohara, I. Uno, and M. Hayasaki and H. Tanimoto, "Influence of meteorological variability on interannual variations of the springtime boundary layer ozone over Japan during 1981–2005," *Atmospheric Chemistry and Physics*, Vol 9, 2009, pp. 6287–6304.
- [31] J. Kurokawa, T. Ohara, I. Uno and M. Hayasaki, "Analysis of episodic pollution of photochemical ozone during 8–9 May 2007 over Japan using the nesting RAMS/CMAQ modeling system," *Japan Society for Atmospheric Environment*, Vol. 43, 2008, pp. 209–224.
- [32] M. Hayasaki, T. Ohara, J. Kurokawa and I. Uno and A. Shimizu, "Episodic pollution of photochemical ozone during 8–9 May 2007 over Japan: Observational data analysis," *Japan Society for Atmospheric Environment*, Vol. 43, 2008, 225–237 (in Japanese).
- [33] E. Saikawa, J. Kurokawa, M. Takigawa, D. L. Mauzerall, L. W. Horowitz and T. Ohara, "The impact of China's vehicle emissions on regional air quality in 2000 and 2020: A scenario analysis" *Atmospheric Chemistry and Physics Discussion*, Vol. 11, 2011, pp. 13141–13192.
- [34] G. A. Grell, S. E. Peckham, R. Schmitz, S. A. McKeen, G. Frost, W. Skamarock and B. Eder, "Fully coupled "online" chemistry within the WRF model," *Atmospheric Environment*, Vol. 39, 2005, pp. 6957-6975.
- [35] M. L. Wesley, "Parameterization of surface resistance to gaseous dry deposition in regional numerical models," *Atmospheric Environment*, Vol. 16, 1989, pp. 1293–1304.
- [36] S. Madronich and S. Flocke, "The role of solar radiation in atmospheric chemistry," *Handbook of Environmental Chemistry*, (P. Boule, ed.), Springer-Verlag, Heidelberg, 1999, pp. 1-26.
- [37] X. Tie, S. Madronich, S. Walters, R. Zhang, P. Rasch, and W. Collins, "Effect of clouds on photolysis and oxidants in the troposphere," *Journal of Geophysical Research: Atmosphere*, Vol. 108 (D20), 2003, 4642, doi:10.1029/2003JD003659.
- [38] J. S. Chang, F. S. Binkowski, N. L. Seaman, J. N. McHenry, P. J. Samson and et al., "The regional acid deposition model and engineering model," *NAPAP SOS/T Report*, Washington DC, Vol. 4, 1989.
- [39] B. Schell, I. J. Ackermann, H. Hass, F. S. Binkowski, and A. Ebel, "Modeling the formation of secondary organic aerosol within a comprehensive air quality model system," *Journal of Geophysical Research: Atmosphere*, Vol. 106, 2001, pp. 28275-28293.
- [40] BBC News: S Korea Bid to Solve Sea Dispute, 2007. Available online: <http://news.bbc.co.uk/2/hi/asia-pacific/6240051.stm> (accessed on 8 January 2007).
- [41] MFAT (The Ministry of Foreign Affairs and Trade, Republic of Korea): Report on the Progress in Consultations on the Naming of the Sea Area between the Korean Peninsula and the Japanese Archipelago. In Proc. Ninth UN Conference on the Standardization of Geographical Names; United Nations Economic and Social Council: New York, NY, USA, 21–30 August, 2007; E/CONF.98/CRP.81.
- [42] W. A. David, N. Ashby and C. C. Hodge, "The Science of Timekeeping. Hewlett-Packard; Application Note No. 1289; Allan's Time Interval Metrology Enterprise: Fountain Green, UT, USA, 1997.

- [43] Y. Hanado, K. Imamura, N. Kotake, F. Nakagawa, Y. Shimizu, R. Tabuchi, Y. Takahashi, M. Hosokawa, T. Morikawa, "The new generation system of Japan standard time at NICT," *International Journal of Navigation and Observation*, 2008, doi:10.1155/2008/841672.
- [44] F. S. Binkowski and U. Shankar, "The regional particulate matter model, 1. Mode description and preliminary results. *Journal of Geophysical Research: Atmosphere*, Vol. 100, 1995, pp. 26191–26209.
- [45] A. B. Guenther, P. R. Zimmerman, P.C. Harley, R. K. Monson, R. Fall, "Isoprene and monoterpene emission rate variability: Model evaluations and sensitivity analyses," *Journal of Geophysical Research: Atmosphere*, Vol. 98, 1993, pp. 12609–12617.
- [46] A. Guenther, P. Zimmerman and M. Wildermuth, "Natural volatile organic compound emission rate estimates for US woodland landscapes," *Atmospheric Environment*, Vol. 28, 1994, pp. 1197–1210.
- [47] W. C. Skamarock, J. B. Klemp, J. Dudhia, D. O. Gill, D. M. Barker, W. Wang and J. G. Powers, "A Description of the Advanced Research WRF Version 2; TN-468tSTR," NCAR: Boulder, CO, USA, NCAR Technical note, 2005, pp. 88.
- [48] S. Y. Hong, J. Dudhia, S. H. Chen, "A revised approach to ice microphysical processes for the bulk parameterization of clouds and precipitation," *Journal of American Meteorological Society*, Vol. 132, 2004, pp. 103–120.
- [49] A. S. Monin and A. M. Obukhov, "Basic laws of turbulent mixing in the surface layer of the atmosphere," *Geophysical Institute of Slovak Academy of Science*, Vol. 151, 1954, pp. 163-187 (in Russian).
- [50] H. H. Shin, S. Y. Hong, J. Dudhia and Y. J. Kim, "Orography-induced gravity wave drag parameterization in the global WRF: Implementation and sensitivity to shortwave radiation schemes," *Advance in Meteorology*, 2010, doi:10.1155/2010/959014.
- [51] J. Dudhia, "Numerical study of convection observed during the winter monsoon experiment using a mesoscale two-dimensional model," *Journal of Atmospheric Sciences*, Vol. 46, 1989, pp.3077–3107.
- [52] E. J. Mlawer, S. J. Taubman, P. D. Brown, M. J. Iacono, S. A. Clough, "Radiative transfer for inhomogeneous atmosphere: RRTM, a validated correlated-k model for the long wave" *Journal of Geophysical Research: Atmosphere*, Vol. 102, 1997, pp. 16663–16682.
- [53] Z. I. Janjic, "The step-mountain coordinate: Physical package," *Monthly Weather Review*, Vol. 118, 1990, pp. 1429–1443.
- [54] Z. I. Janjic, "The step-mountain ETA coordinate model: Further development of the convection, viscous sub-layer, and turbulent closure schemes," *Monthly Weather Review*, Vol. 122, 1994, pp. 927–945.
- [55] M. B. Ek, K. E. Mitchell, Y. Lin, E. Rogers, P. Grunmann, V. Koren, G. Gayno, J. D. Tarpley, "Implementation of Noah land surface model advances in the National Centers for Environmental Prediction operational mesoscale Eta model," *Journal of Geophysical Research: Atmosphere*, Vol. 108, 2003, pp. 8851–8867.
- [56] W. R. Stockwell, P. Middleton, J. S. Chang, "The second generation regional acid deposition model chemical mechanism for regional air quality modeling," *Journal of Geophysical Research: Atmosphere*, Vol. 95, 1990, pp. 16343–16367.
- [57] S. Madronich, "Photodissociation in the atmosphere 1. Actinic flux and the effects of ground reflections and clouds," *Journal of Geophysical Research: Atmosphere*, Vol. 92, 1987, pp. 9740–9752.
- [58] S. R. Freitas, K. M. Longo, M. F. Alonso, M. Pirre, V. Marecal, G. Grell, R. Stockler, R. F. Mello, G. M. Sanchez, "PREP-CHEM-SRC 1.0: a preprocessor of trace gas and aerosol emission fields for regional and global atmospheric chemistry models," *Geoscientific Model Development*, Vol. 4, 2011, pp. 419-433.
- [59] M. Schultz, "RETRO team. RETRO Emission Trends and Variability," Presented at 1st ACCENT Symposium, Urbino, Italy, 12–16 September, 2005. Available online: <http://retro.enes.org/index.shtml> (accessed on 8 April 2008).
- [60] C. Granier, U. Niemeir, J. F. Muller, J. Olivier, J. Peters, A. Richter, H. Nuss and J. Burrows, "Variation of the Atmospheric Composition over the 1990–2000 Period," EU project EVK2-1999-00011, Report No. 6; POET: Paris, France, 2003.

- [61] J. Olivier, J. Peters, C. Granier, G. Petron, J. F. Muller, S. Wallens, "Present and Future Surface Emissions of Atmospheric Compounds," EU project EVK2-1999-00011, POET report No. 2; POET: Paris, France, 2003.
- [62] J. G. J. Olivier, J. P. J. Bloos, J. J. M. Berdowski, A. J. H. Visschedijk and A. F. Bouwman, "A 1990 global emission inventory of anthropogenic sources of carbon monoxide on 1×1 developed in the framework of EDGAR/GEIA," *Chemosphere: Global Change Science*, Vol. 1, 1999, pp. 1–17.
- [63] J. G. J. Olivier, A. F. Bouwman, C. W. M. Van der Maas, J. J. M. Berdowski, C. Veldt, J. P. J. Bloos, A. J. H. Visschedijk, P. Y. J. Zandveld and J. L. Haverlag, "Description Of EDGAR Version 2.0: A Set of Global Emission Inventories of Greenhouse Gases and Ozone-Depleting Substances for All Anthropogenic and Mos-Natural Sources on a Per Country Basis and On a 1×1 Grid," RIVM report No. 771060 002; RIVM: Bilthoven, The Netherlands, 1996. Available online: <http://www.mnp.nl/edgar/introduction>. (accessed on 5 October 2010).
- [64] J. G. J. Olivier, J. J. M. Berdowski, J. A. H. W. Peters and J. Bakker, A. J. H. Visschedijk, J. P. J. Bloos, "Applications of EDGAR. Including a Description of EDGAR 3.0: Reference Database with Trend Data for 1970–1995," Bilthoven; RIVM report no. 773301 001/ NOP report no. 410200 051; RIVM: Bilthoven, The Netherlands, 2001.
- [65] G. R. Van der Werf, J. T. Randerson, G. J. Collatz, L. Giglio, P. S. Kasibhatla, A. Avelino, S. C. Olsen, E. S. Kasischke, "Continental-scale partitioning of fire emissions during the 1997–2001 El Nino/La Nina period," *Science*, Vol. 303, 2004, pp. 73–76, 2004. Available online: http://daac.ornl.gov/VEGETATION/guides/global_fire_emissions_v2.1.html. (accessed on 22 June 2010).
- [66] G. R. Van der Werf, J. T. Randerson, L. Giglio, G. J. Collatz and P. S. Kasibhatla, "Interannual variability in global biomass burning emission from 1997 to 2004," *Atmospheric Chemistry and Physics*, Vol. 6, 2006, pp. 3423–3441.
- [67] R. J. Andres, D. J. Fielding, G. Marland, T. A. Boden and N. Kumar, "Carbon dioxide emissions from fossil-fuel use 1751-1950" *Tellus*, Vol. 51B, 1999, pp. 759-765.
- [68] NIES (National Institute for Environmental Studies). Observation Data Download for Pollutant Concentration in the Atmospheric Environment. Available online: http://www.nies.go.jp/igreen/td_down.html (accessed on 20 July 2010) (in Japanese).
- [69] KCAPMC (Kawasaki City Air Pollution Monitoring Centre). Air pollutant monitoring data can be downloaded from the website: http://www.city.kawasaki.jp/30/30kansic/home/en/e_index.htm (accessed on 1 October 2010).
- [70] H. Akasaka and H. Nimiya, "A method to estimate the hourly solar radiation using AMeDAS data," Departmental Bulletin Paper, Kagoshima University Faculty of Engineering Report (in Japanese), Report No. 28/1986, 99-116, 1986. Available from: http://ir.kagoshima-u.ac.jp/bitstream/10232/11379/1/AN00040363_v28_p99-116.pdf (accessed on 1 November 1986).
- [71] E. Velasco, C. M. Arquez, E. Bueno, R. M. Bernabe, A. S. Anchez, O. Fentanes, H. W. Ohnschimmel, B. C. Ardenas, A. Kamilla, S. Wakamatsu and L. T. Molina, "Vertical distribution of ozone and VOCs in the low boundary layer of Mexico City," *Atmospheric Chemistry and Physics Discussion*, Vol. 7, 2007, pp. 12751–12779.
- [72] USEPA (United States Environmental Protection Agency). Technology Transfer Network OAR Policy and Guidance. Federal Register / Vol. 70, No. 63 / Monday, April 4, 2005 / Proposed Rules Available online: http://www.epa.gov/ttn/oarpg/t1/fr_notices/3866finalfrnotice.pdf (accessed on 25 March 2005).
- [73] C. E. Sioris, J. Zou, C. T. McElroy, C. A. McLinden and H. Vomel, "High vertical resolution water vapour profiles in the upper troposphere and lower stratosphere retrieved from MAESTRO solar occultation spectra," *Advance in Space Research*, Vol. 46, 2010, pp. 642–650.
- [74] B. J. Finlayson-Pitts and J. Finlayson-Pitts, "Chemistry of the Upper and Lower Atmosphere: Theory, Experiments and Applications," Academic Press, Inc., Academic Press, San Diego, CA, London, 2000.
- [75] X. Tie, S. Madronich, G. H. Li, Z. M. Ying, R. Zhang, A. Garcia, J. Lee-Taylor, Y. Liu, "Characterizations of chemical oxidants in Mexico City: a regional chemical/dynamical model (WRF/Chem) study," *Atmospheric Environment*, Vol. 41, 2007, pp. 1989–2008.

- [76] D. P. Lalas, M. Tombroutsella, M. Petrakis, D. N. Asimakopoulos and C. Helmis, "An experimental study of the horizontal and vertical distribution of ozone over Athens," *Atmospheric Environment*, Vol. 21, 1987, pp. 2681-2693.
- [77] R. Lu and R. P. Turco, "Air pollutant transport in a coastal environment. Part I. Two dimensional simulations of sea-breeze and mountain effects," *Journal of Atmospheric Science*, Vol. 51, 1994, pp. 2285-2308.
- [78] M. M. Millan, L. Alonso, J. A. Legarreta, M. V. Albizu and I. Ureta, "A fumigation episode in an industrialized estuary: Bilbao, November 1981," *Atmospheric Environment*, Vol. 18, 1984, pp. 563-572.
- [79] M. M. Millan, B. Artinano, L. Alonso, M. Castro, R. Fernandez-Patier and J. Goberna, "A Meso-Meteorological Cycles of Air Pollution in the Iberian Peninsula (MECAPIP)," *Air Pollution Research Report*, Vol. 44, 1992, EUR No. 14834, EC DG XII/E'1, Brussels, Technical report.
- [80] N. Ahmad and J. Linderman, "A godunov type finite volume scheme for meso- and micro-scale flows in three dimensions," *Pure and Applied Geophysics*, Vol. 165, 2008, 1929–1939.
- [81] M. Baldauf and W. C. Skamarock, "An Improved Third Order Vertical Advection Scheme for the Runge-Kutta Dynamical Core," In *Proceedings of 8th International SRNWP-Workshop on Non-Hydrostatic Modelling*, Bad Orb, Germany, 26–28 October, 2009.
- [82] G. A. Grell and D. Devenyi, "A generalized approach to parameterizing convection combining ensemble and data assimilation techniques," *Geophysical Research Letter*, Vol. 29, 2002, doi:10.1029/2002GL015311.



Khandakar Md. Habib Al Razi is a Postdoctoral Researcher in the Environmental and Renewable Energy Systems (ERES) division, Graduate School of Engineering, Gifu University, Japan. He has long experience to work on atmospheric dispersion modelling from coal combustion facilities in Japan. He has obtained his B.Sc. Engineering in Chemical Engineering from Bangladesh University of Engineering and Technology (BUET), Dhaka, Bangladesh in 2004. He obtained his Master's degree in 2010 and Doctoral degree in 2013 in Environmental and Renewable Energy System (ERES), Graduate School of Engineering, Gifu University, Japan. Currently he is working on energy and meteorological modelling and air quality modelling by using WRF and WRF-CHEM model.
E-mail address: habibalrajii@yahoo.com



Moritomi Hiroshi is a Professor in the Environmental and Renewable Energy Systems (ERES) division, Graduate School of Engineering, Gifu University, Japan. He was born in Aichi Prefecture, Japan. He received his Undergraduate degree in 1977 and Master's degree in 1979 in Nagoya Institute of Technology. He obtained Ph.D degree from Hokkaido University, Japan. 1980 he joined Hokkaido University as Research Assistant. 1987 he joined in Ohio State University as a Researcher. 1988 he joined in the National Institute of Advance Industrial Science and Technology (AIST). 1995 he was appointed in ERES of Gifu University as Associate Professor and 1999 he obtained promotion as Professor. Prof. Moritomi is a member of Japan Society of Chemical Engineers, Japan Institute of Energy, Combustion Society of Japan, Japanese Society for Multiphase Flow, Heat Transfer Society of Japan, Japan Society of Mechanical Engineers, Society of Waste Recycling, Japan Association of Aerosol and many other local and international societies. He has published many articles in peer reviewed national and international journals. He has organized several symposia, workshops, etc. as also chaired a number of technical sessions of national/international events on his relevant field. He is carrying out many projects related to his research work. He was awarded the Progress Energy Society of Japan Award in 1996, Best Paper Award 6th International Conference on High Temperature Gas Purification in 2005, Energy Society of Japan Award in 2006, Japan Institute of Energy Award in 2010, Energy Society of Japan Award in 2011.
E-mail address: moritomi@gifu-u.ac.jp, Tel: +81-293-2591